ADVANCED PHOTONICS RESEARCH
Open Access
www.adpr-journal.com

Impact of Attaching Selectively Reflecting Cholesteric Layers on Edge Output of Static and Dynamic Luminescent Solar Concentrators

*Sebastian J. M. Robben, Pietro Commessatti, Ece Taşan, Gianmarco Griffini, and Michael G. Debije**

Luminescent solar concentrators offer a versatile option for renewable electricity generation for deployment in the built environment. The primary challenge of these devices remains the reduction of various losses that limit them to modest efficiencies. Wavelength-selective chiral nematic (cholesteric) liquid crystal reflectors with air gaps are found to yield promising results in the past, reducing surface losses and increasing edge emissions. Herein, the influence of directly attached cholesteric reflectors on the edge outputs of both static and switchable "smart window" luminescent solar concentrator lightguides is investigated. For lightguides containing a coumarin dye, an increase in edge photon emission of at least 30% (from 2.2% to 2.9% external photon efficiency) is achieved when using full reflectors at both top and bottom of both static and dynamic lightguides with a central reflection wavelength centered at 600 nm, ≈70 nm red-shifted to the dye emission peak.

1. Introduction

Solar energy systems have become an important staple of renewable energy alternatives to fossil fuels.[1] Conventional solar energy systems using photovoltaic (PV) cells show numerous useful advantages over other renewable energy sources; the electrical generation can be made close to the user, it is noiseless and low cost in operation and maintenance.[2] The luminescent solar concentrator (LSC) has been proposed to complement standard PV technologies specifically for deployment in urban settings.[3–7] Typical LSCs consist of a plastic or glass sheet topped with or impregnated by luminescent dye molecules. The dyes absorb both incident direct and indirect sunlight and re-emit the absorbed energy at longer wavelengths, a significant fraction of the light directed in such a way as to be trapped by total internal reflection (TIR) in the plastic or glass sheet which acts as a lightguide. LSCs may be produced in any color (or colorless),[8] shape,[9] and size,[10] allowing for easier urban integration as street furniture,[11] bicycle shelters,[11] noise barriers,[10] windows,[12–15] or as building facades,[7] where color is ubiquitous to the urban environment.[16–18] The trapped light can be used to illuminate edge-mounted PVs for generation of electricity,[3,19] hydrogen,[20] or emission can be used directly to drive photochemical reactions.[21] By embedding a fluorescent dye in a host liquid crystal (LC), it is possible to make 'smart' windows that can switch between a "dark" state that absorbs incident light, the dyes re-emitting this light at a longer wavelength so as to be trapped within the glass plates for generating electricity, and "light" states where the dye absorbs minimal light.[22,23]

Despite the lightguiding, a significant fraction of the emission light is not trapped by TIR and is emitted through the surfaces of the lightguide: losses generally are 30%–50% of dye emitted light.[24] While this surface loss can be utilized for spectral downshifting in PVs,[25] or in horticulture to enhance plant growth,[26,27] in most LSC-based devices, surface losses are undesirable, as they represent losses of potential photons reaching the PV at the device edges, and thus loss in efficiency.

Several attempts have been made to confine the LSC emission light to the lightguide. Alignment of the dichroic dyes provides one manner of control of the emission, with homeotropic alignment essentially eliminating surface loss, but also severely restricting the possibility of the system absorbing light.[28–30] Alternative antenna dye designs allow capture of light from one luminophore, and emission by another favorably oriented for light capture, but such dyes would be quite expensive.[31–34]

S. J. M. Robben, E. Taşan, M. G. Debije
Stimuli-responsive Functional Materials and Devices
Department of Chemical Engineering and Chemistry
Eindhoven University of Technology
P.O. Box 513, Eindhoven 5600 MB, The Netherlands
E-mail: m.g.debije@tue.nl

P. Commessatti, G. Griffini
Department of Chemistry
Materials and Chemical Engineering "Giulio Natta"
Politecnico di Milano
Piazza Leonardo da Vinci 32, 20133 Milano, Italy

M. G. Debije
Eindhoven Institute of Renewable Energy Systems (EIRES)
Eindhoven University of Technology
P.O. Box 513, Eindhoven 5600 MB, The Netherlands

The ORCID identification number(s) for the author(s) of this article can be found under https://doi.org/10.1002/adpr.202500122.

DOI: 10.1002/adpr.202500122

Another approach to reduce surface losses is using selectively-reflecting mirrors transparent to wavelengths absorbed by the dye and reflective to wavelengths emitted by the dyes (see **Figure 1**). Previous efforts have used Bragg reflectors,[35–37] silver and aluminum metal films,[38] photonic layers,[39] and rugate filters.[40]

Generally, organic Bragg reflectors are difficult to extrude, and metallic reflectors are tedious to deposit. A class of selective reflector much more easily deposited from solution is chiral nematic (cholesteric) liquid crystals (ChLCs). ChLCs are nematic LCs which have been doped with a chiral molecule.[41] The chiral dopant induces a 'twist' between the adjacent LC layers, forming a helical structure. This helix can either be right- or left-handed (RH, LH) depending on the nature of dopant used and reflects a bandwidth of light of the same polarization handedness as the helix, meaning a RH-ChLC reflects RH-circularly polarized light (CPL), and vice versa, with bandwidth $\Delta\lambda$ determined by

$$\Delta\lambda = \Delta np \tag{1}$$

where Δn is the difference between the extraordinary and ordinary refractive indexes of the LC host, and p the pitch, defined as the distance it takes for the helix to undergo a 360° turn (typically resulting in a bandwidth on the order of 50–75 nm in the visible range). The pitch is related to the helical twisting power (HTP) of the chiral dopant, a measure of the ability of a chiral dopant to induce the helical structure in the nematic LC. A stronger HTP will result in a shorter pitch and, in turn, the ChLC reflecting shorter wavelengths. The chiral dopant weight concentration C_w determines the pitch and reflected wavelength, summarized by equation[42]

$$\mathrm{HTP} = \frac{1}{c_w p} \tag{2}$$

Since a ChLC can either reflect RH- or LH CPL, a combination of two ChLC reflectors is needed to fully reflect sunlight of a specific wavelength. To fully minimize surface losses, these full reflectors need to be applied on both sides of the lightguide to retain the translucent property of the LSC panel, which is a sought-after characteristic in many applications in the built environment (e.g., windows).

Our initial work on using ChLC reflectors employed two RH-ChLC layers deposited on either side of a halfwave plate, which was laid atop an LSC lightguide with a scatterer at the bottom.[43,44] While the ChLCs were demonstrated to be effective, the system was not always applicable as the devices had an air gap between the lightguide and the ChLC layer which could easily be fouled and/or easily torn away by the wind, and the device was not transparent as it used a rear scatterer. In this work, we directly attach RH- and LH-ChLC reflective layers to the top and bottom surfaces of both static and dynamic LSCs, allowing translucent devices with improved performance over device employing reflective layers and an air gap, with a significant blue shift in the wavelength of the most effective reflection band.

2. Experimental Section

The static LSC lightguides were made from a solution consisting of a pentaacrylate/methyl methacrylate mixture (70:30 weight ratio, Polysciences Inc), 1 wt% of the photoinitiator Irgacure 184 (Ciba), and 0.25 wt% of DFSB-K160 (K160), a fluorescent coumarin-derivate (Risk Reactor) spincoated on $50 \times 50 \times 5\ \mathrm{mm}^3$ polymethyl methacrylate plates (PMMA, Plano Plastics) at 1000 rpm for 30 s and immediately placed under a low-intensity Philips UV lamp at room temperature in a nitrogen atmosphere for 10 min to photopolymerize. The dynamic lightguides used 0.1 wt% K160 dye in the commercial LC mix E7 (Merck) to fill custom $50 \times 50 \times 5\ \mathrm{mm}^3$ ITO cells (LCtec) with spacers to form a 20 μm between the plates with planar alignment layers at 60 °C by capillary action.

Prior to coating lightguides with RH-ChLC layers, an alignment layer of 5 wt% polyvinyl alcohol (PVA 87%–89% hydrolyzed, Mw 31 000–50 000, Sigma-Aldrich) in water was spincoated at 1000 rpm for 30 s on top of the dye layer (static samples) or one side of the glass cells (dynamic samples) and placed on a hotplate at 90 °C for ≈10 min to ensure all water evaporated. The lightguides and cells were removed from the hotplate and left to cool to room temperature. The PVA layer was then rubbed on a rubbing cloth two times, exerting moderate and uniform pressure. After the rubbing, a solution consisting of the liquid crystal Paliocolor LC242 (BASF) with varying concentrations of the chiral dopant LC756 (BASF; HTP in LC242 calculated to be $\approx 64\ \mu\mathrm{m}^{-1}$), 1 wt% of the photoinitiator Irgacure 184 (Ciba, Basel, Switzerland), and 0.1 wt% of surfactant, 2-(N-ethyl-perfluorooctane sulfonamido) ethyl acrylate (ABC Chemicals), in xylene (55 wt%, Biosolve) was spincoated at 1000 rpm for 30 sec at room temperature; the plates were immediately placed on a hotplate at 80 °C for ≈30 s until the solvent evaporated and the ChLC phase had formed, after which they were photopolymerized under a low-intensity Philips UV lamp ($1\ \mathrm{mW\,cm}^{-2}$) at room temperature for >90 s under nitrogen

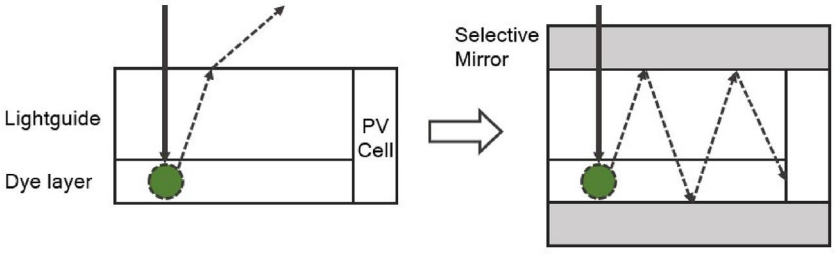

Figure 1. Schematic illustration of the concept of wavelength-selective mirrors and their application on LSC devices. On the left, an initial situation is depicted where emitted light is lost through the surface. On the right, selective mirrors are applied on top and bottom of the lightguide, reflecting otherwise lost light, allowing it to exit the edge of the device. Layers are not shown to scale.

atmosphere. The opposite side of each plate or cell was coated with PVA and rubbed on a cloth, after which the same ChLC solution was spread using a spin coater under identical conditions, and after heating to the nematic phase and cooling to room temperature and then photopolymerized, resulted in lightguides with identical RH-ChLC layers on each face.

LH-ChLC layers were added on top of the existing right-handed reflectors. One lightguide side was spincoated with 5 wt% PVA solution and rubbed and spincoated with a solution similar to those used for the righthanded ChLC layer: liquid crystal LC242, 1 wt% photoinitiator and 0.1 wt% surfactant, and S-*trans*-stilbene oxide (TSO, internally synthesized; HTP~ $-27\ \mu m^{-1}$ in LC242) at various weight concentrations in xylene (55 wt% solution; 99% pure, Biosolve). After application of the left-handed ChLC on one side of the lightguide, a PVA layer was applied to the opposite face, rubbed, after which the same LH-ChLC solution was coated on the rubbed PVA, heated to the nematic state, cooled, and photopolymerized. In some samples, the left-handed layers were applied before the right-handed. An illustration of the device construction is given below as **Figure 2**.

Absorption and transmission spectra were recorded on a Shimadzu UV-3102 spectrophotometer. Edge emission for each of these samples was measured using an SLMS 1050 integrating sphere (Labsphere) equipped with a diode array (RPS900, International Light, sensitive to a spectral range of 350 to 1000 nm) exposed to AM1.5 G spectrum from a 300 W solar simulator light source (Scisun, Figure S1 in the supplemental information (SI)). The solar simulator light is ≈7% polarized perpendicular to the sphere entry point: the results in this work were not corrected for this anisotropy, so the edge emission ratios reported for the aligned cells may be considered minimum values. The top surfaces of the static lightguides were illuminated while being securely held in place by an anodized aluminum holder (measured reflection ≈7%) and the switchable cells on a 3D printed polymer holder coated with matte black spray paint (also ≈7% reflectivity; see Figure S2, Supporting Information), with the lightguide edge of interest facing toward the integrating sphere. All the measurements of static samples were done with the dye-coated side facing away from the incident light (e.g., placed at the bottom), and all emission edges were measured. To make representative comparisons with the subsequent samples coated with ChLC layers, the first edge measured was indicated with a dot. In total, 11 identically-prepared samples coated only with K160 with 44 sides measured showed total emission variations of 3.7%. For the dynamic cells, edge emissions were possible from two edges, one with alignment layer parallel to the integrating sphere port, and one with alignment layers perpendicular. Square wave, 1000 Hz electric potentials were applied to the cells via a BK Precision 4054B function generator and alligator clips.

3. Results and Discussion

The absorbance spectra of static $50 \times 50 \times 5$ mm[3] PMMA LSCs coated with 0.25 wt% of the model fluorescent dye K160 (fluorescence quantum yield ≈97% in a liquid crystal environment[45]) in an acrylate host were recorded, and emission from each of the four edges under AM1.5 G illumination was measured using an integrating sphere (see both the absorbance and emission spectra of the LSC shown in **Figure 3**). While the K160 dye is not robust enough to withstand continual outdoor exposure, it serves as a good model system durable enough to withstand the exposures experienced in these experiments over the short exposure times they experienced during the experiments (<10 min total exposure; see Figure S3, Supporting Information) and very soluble in the host materials. The calculated η_{int} (internal photon efficiency, a measure of the number of photons emitted as a fraction of number of photons absorbed) for the LSC was estimated to be 75.6% (see Table S1, Supporting Information).[46,47]

We then applied RH-ChLCs to LSCs with reflection wavelengths centered at 470, 530, 600, 650, 700, or 800 nm on both the top and bottom surfaces of the lightguides (that is, a RH-ChLC layer on a rubbed PVA layer on top of the dye-doped layer and a RH-CLC film on a rubbed PVA layer on the opposite face of the LSC), and the resulting edge emissions measured. The 470 nm reflection band significantly overlaps the absorption spectrum of the coumarin-derivative dye, while 530 nm largely coincides with the peak emission (**Figure 4**a).

Finally, we added wavelength matching LH-ChLCs on top of PVA alignment layers atop the RH-ChLCs on both sides of the lightguide and again measured all four edge outputs (Figure 4b). One such collection of emission spectra from one sample edge is

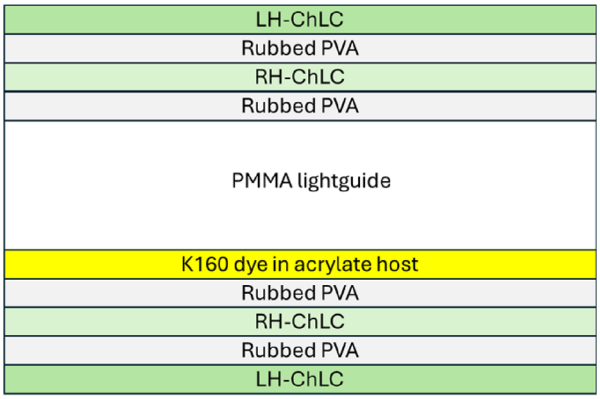

Figure 2. Schematic of the structure of the static LSC devices; layer thicknesses not to scale.

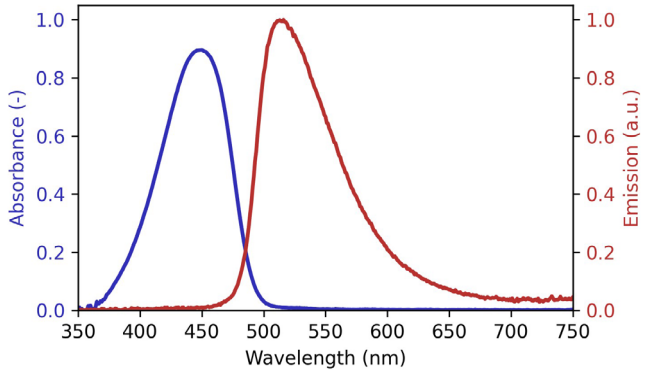

Figure 3. Absorption (blue line) and normalized edge emission (red line) spectra of a lightguide coated with 0.25 wt% K160 dye in an acrylate host.

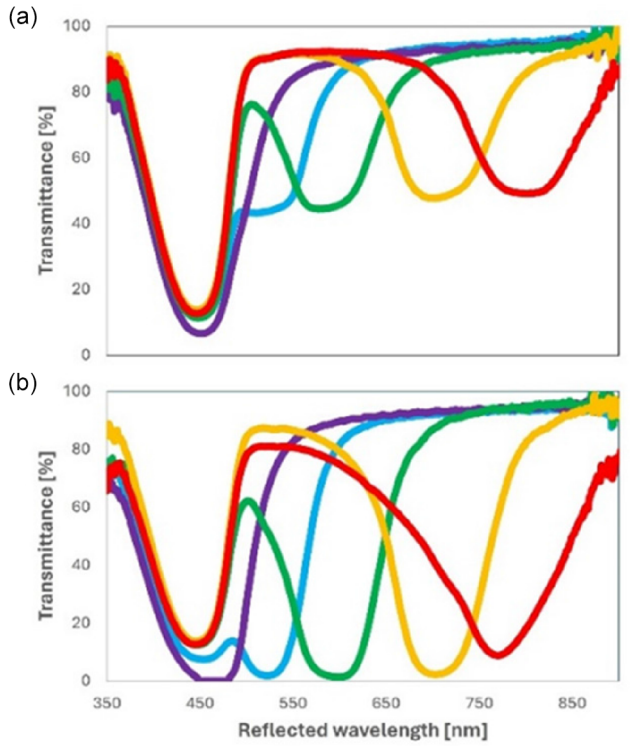

Figure 4. Reflection spectra for a) RH-ChLCs using chiral dopant concentrations of 5.3 wt% (violet), 4.7 wt% (blue), 4.1 wt% (green), 3.5 wt% (orange), and 3.1 wt% (red) LC756 and b) stacked RH- and LH- (11.6 wt%, 10.4 wt%, 9.2 wt%, 7.7 wt%, 7 wt% TSO) ChLCs. The prominent peak at ≈450 nm results from the absorbance by the 0.25 wt% K160 dye layer.

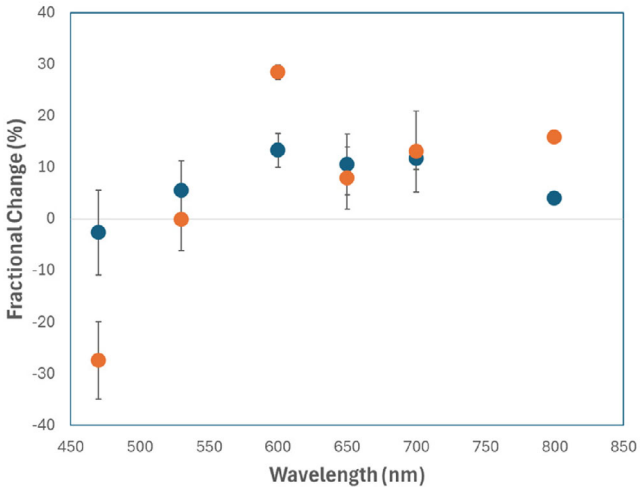

Figure 5. Fractional change in edge emission of photons from 0.25 wt% K160 topped lightguides after application of a single, RH-ChLC to both front and back sides (blue) and application of a LH-ChLC on the RH-ChLC films (orange). Error bars refer to measurements of two samples at each wavelength ≤700 nm. The performance of a bare LSC with no attached cholesteric is indicated by the dotted line.

shown as Figure S4 in the Supplemental Information. We convert the energy of emission at each wavelength into number of photons, n_λ, by using

$$E_\lambda = n_\lambda hc/\lambda \tag{3}$$

where E_λ is the measured energy at the wavelength λ, h is Planck's constant (6.626×10^{-34} Js), and c is the speed of light (2.998×10^8 ms^{-1}). To determine edge output, we integrated the emission spectra over the range of emission wavelengths, which we took to be 450–750 nm.

The relative results of the emission measurements are depicted in **Figure 5**. While the measured edge emissions from the dye-topped lightguides without ChLCs were reproducible, there were more variations in the results after adding the ChLC liquid crystal layers: this may be expected due to the multiple steps involved preparing the samples (eight layers in total on the dye-topped lightguide). Despite this, the results are reasonably consistent, and while absolute values of single samples may vary, the general trend is quite clear. Because of the uncertainty of determining the exact dye absorption with the attachment of the cholesteric layers, we refrain from reporting an internal photon efficiency for the coated devices.

It is obvious employing a cholesteric with reflection band centered too close to the absorption wavelength negatively or minimally affects the emission of light to the edge of the lightguide. The dual-reflector centered at 600 nm, red-shifted some ≈70 nm from the peak emission around 530 nm, generated up to 30% higher edge emission than the bare LSC lightguide. An even greater red-shifted reflector from the peak emission wavelength for the sample with the best performance was seen in previous work using ChLC reflectors with an air gap.[43] Since the dye used in the previous work using an air gap, Lumogen Red 305, is quite different than the dye used in this work, and the previous work deployed a rear scatterer rather than the blackened surface used here, direct comparisons must be made with caution. The previous work showed a peak emission increase at equivalent peak absorbance values (≈90% absorption) of 15% using a ChLC shifted some 150 nm from the emission peak.[43] Initial indications are by attaching the reflectors directly to the lightguide, the most effective reflector is less red-shifted from the peak emission wavelength. With an attached reflector, the effectiveness of the cholesteric layer appears to double with respect to previous work.

The sun is not stationary, and so consideration must also be taken for the relative position of the incident light to the LSC ChLC layer. Light incident at an angle with respect to the ChLC normal encounters a blue-shifted reflective wavelength, which consequently may cause incident light to be reflected away before it may enter the lightguide for absorption.[48] To study this impact, we took three LSC lightguides coated with full reflectors on both sides of the lightguide centered at 470, 530, and 700 nm and measured their emission on the integrating sphere by rotating the sample holder. The edge emission at incidence angles of 20, 30, 45, and 60° to the lightguide surface normalized to the sample's emission at normal incidence is reported (see **Figure 6**). The black dotted line represents the theoretical impact of the rotation of the sample simply based on the reduced surface area relative to the light source. The results are as one might

expect. The edge emission of the sample with the 470 nm reflector immediately drops sharply upon increasing the angle, a result of the reflection band shifting into the absorbance spectra of the dye. This is also the case for the 530 nm sample, but the effect is less rapid as the reflector starts around the peak emission of the dye. The 700 nm sample shows a quite different impact, actually increasing the performance slightly at steeper angles, likely an effect of increased pathlength of light through the dye layer for enhanced absorption. The take-home message is that for the LSC, a red-shifted reflection band provides the best balance between capturing surface losses and maintaining emission light in the lightguide and avoiding losses of incident light at steeper angles.

The absorption spectra of 20 µm ITO-coated cells filled with 0.1 wt% K160 dye in the E7 LC host were taken with light polarized both parallel ($A_{||}$) and perpendicular ($A_{\perp}$) to the alignment direction of the host LCs. As expected, there is a more pronounced impact on the absorption spectra when the light is polarized parallel to the host LC than perpendicular, suggesting the fluorescent dye is aligned predominantly parallel to the host LC: the order parameter, S, determined by

$$S = \frac{(A_{||} - A_{\perp})}{(A_{||} + 2A_{\perp})} \tag{4}$$

was calculated to be 0.49–0.52, in line with previous results for this dye in this host.[22] By applying electrical potential across the cell, the average tilt angle of the K160 dye could be modified, resulting in decreased absorbance for light polarized parallel to the alignment direction of the dye (Figure S5, Supporting Information). The average tilt angles of the dyes with respect to the surface were estimated by assuming all molecules lay flat at no applied field and absorb geometrically less light with increasing angle: the calculated tilts may be seen in Table S2, Supporting Information. The calculated internal photon efficiency (number of photons emitted as a fraction of calculated total absorbed photons 350–1000 nm; absorbed photons were determined by combining the solar simulator spectrum and the dye absorption spectrum, and we did not adjust for the ≈7% of photons reflected from the LSC sample holders during illumination so reported internal photon efficiencies can be assumed as maxima) photon efficiencies of the LSC cell as a function of applied potential are shown in **Table 1**.

Applying the eight layers necessary to produce full reflectors on either side of the cell (four PVA alignment layers and two each of left- and right-handed reflector) was a challenging process, and most of the samples displayed some degree of scatter in the reflectors. Transmission spectra of all the samples are shown in **Figure 7**.

Light emissions from the cell were determined from two orthogonal edges, one parallel and one perpendicular to the alignment of the LC host with RH- and LH-ChLC reflectors applied to both the top and bottom surfaces of the lightguide as a function of applied potential across the cell. Sample edge emission spectra corrected for scattering from the E7 are shown in Figure S6, Supporting Information: corrections were made by matching the 760 and 830 nm spectral features of the solar simulator with corresponding peaks in the emission spectra of the dye and subtracting the scaled simulator spectrum from the edge emission spectrum. The analysis was complicated by the imperfect nature of the handmade cholesteric stacks, with additional light being directly scattered to the edge. While this appears

Table 1. Calculated internal photon efficiencies of a bare K160 LSC cell as a function of applied potential (determined by calculating individual efficiencies from the parallel and perpendicular cell edges and doubling).

Applied potential (V)	0	1	2	3	4	5	6	7	8	9	10
Calculated ηint (%)	57	57	57	60	65	69	72	74	75	76	77

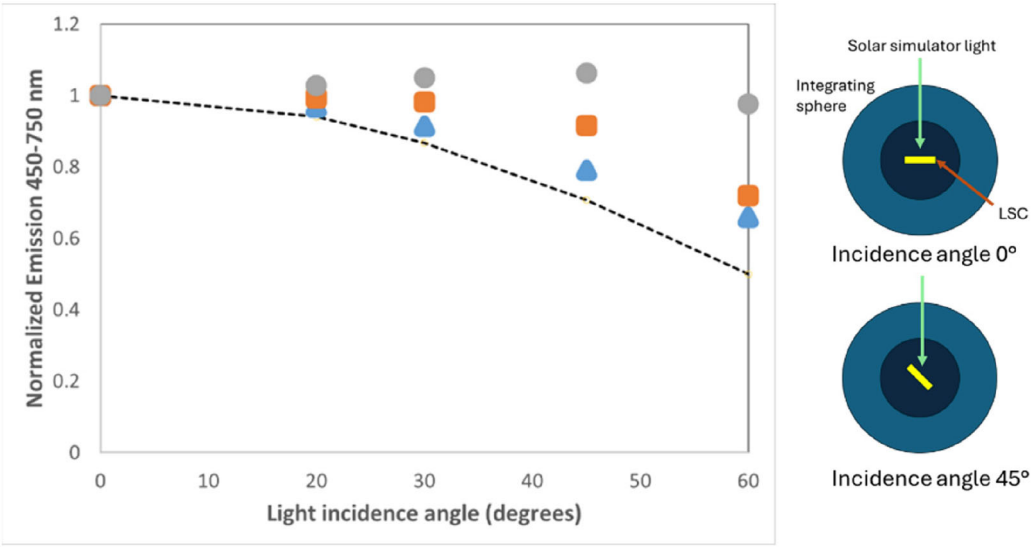

Figure 6. (Left) Normalized edge emissions of samples with (blue triangles) 470 nm, (orange squares) 530 nm, and (gray circles) 700 nm RH- and LH-ChLC layers applied to both top and bottom as a function of incident angle of the solar simulator light to the lightguide surface. (Right) Definition of incidence angle of excitation illumination.

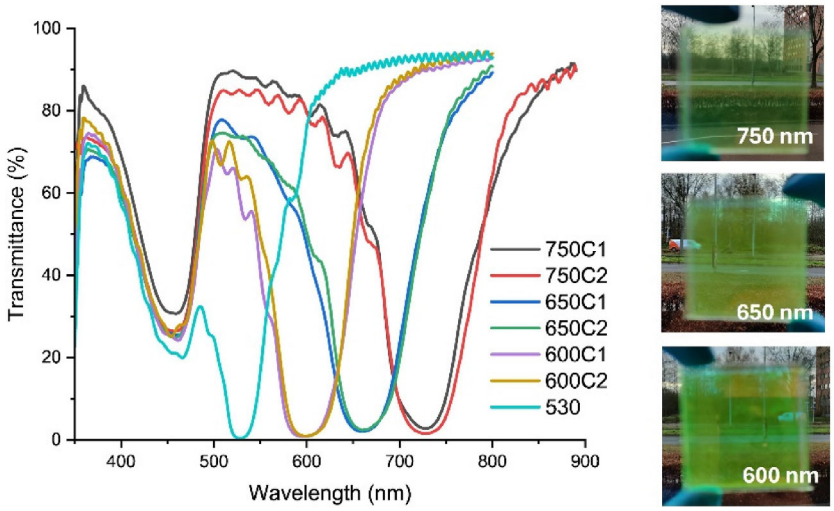

Figure 7. Transmission spectra of all 20 µm ITO cells containing 0.1 wt% K160 in E7 (the peak at around 450 nm) with the ChLC coatings centered at approx. 530, 600, 650, and 750 nm examined in this work. In the legend, numbers refer to the central reflection wavelength of the coating on the cell, while C1 and C2 differentiate them when two separate samples were made. Insets are photographs of the samples 750C2, 650C2, and 600C2.

to enhance the performance of the LSC, it is expected that upon producing industrial-quality cholesterics with no scatter, these effects will disappear. In addition, such scattering effects are quite short range (productive only over a few cm[49]). Based on the edge emission spectra, we have restricted our analysis to the 530 and 600 nm samples: the other samples show a significant impact from the scattering, and while the results give high emission, we do not feel they may be properly compared to the original sample, and proper calculation of actual dye absorption is too uncertain to claim a specific internal photon efficiency. The results of these analyses are found in **Table 2**.

The calculated average fractional edge emission increase for the 600 nm cholesteric reflector stack of around 35% for the switchable LSC is quite similar to the 30% determined for the static LSCs. Edge emissions at each applied potential were also recorded, and the results seen in **Figure 8**. The edge emission photon flux showed an increase upon application of electric potential, as might be expected be the reorientation of the dye to a more vertical position, the dipole emission now preferentially directed into the lightguiding mode.[24] The external photon efficiencies (the number of edge emitted photons as a faction of photons incident on the lightguide surface from 350 to 1000 nm) increased upon application of the electrical potential as well (see **Table 3**).

Table 2. Integrated edge emission for 20 µm 0.1 wt% E7/K160 cells at rest topped with 600 nm, 530 nm, and no cholesteric layers recorded on a holder with a painted black plastic background. Fractional increases in the measured integrated emission over the noncoated (bare K160) cell are also shown.

Cell	Bare K160	600 [nm]	530 [nm]
Perpendicular emission (photons s^{-1}) $\times 10^6$	1.50	2.16	2.07
Increase (%)	–	44	38
Parallel emission (photons s^{-1}) $\times 10^6$	2.00	2.53	2.25
Increase (%)	–	27	12

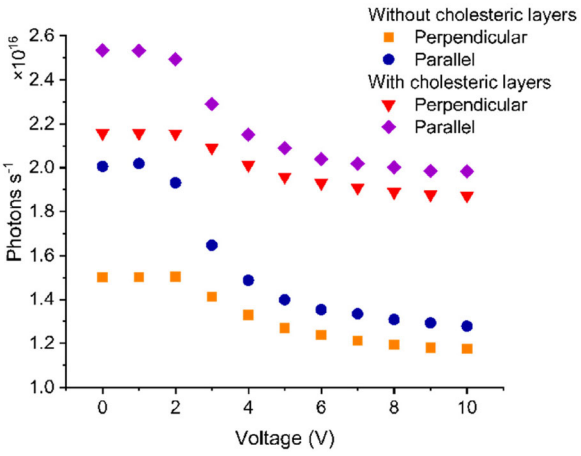

Figure 8. Averaged edge emission (photon flux) with respect to applied potential for the two orientations, parallel (violet) and perpendicular (red) for an LSC cell filled with 0.1 wt% K160 in E7, coated with a ChLC layer with a central reflective wavelength of 600 nm measured on a black background. The data for a noncoated cell are also shown for comparison from parallel (blue) and perpendicular (orange) edges. The values for the LSC cells coated with a 600 nm reflector are an average between the spectra of two cells produced and corrected for LC host/cholesteric scattering.

One possibility for further improving LSC performance is to not only improve the quality of the reflectors, but to reduce the angular dependence of the ChLC.[50] Reducing the angular shift would allow the centering of the reflection more directly in the wavelength range of the emission and reducing the rejection of sunlight incident at steep angles to the lightguide surface. Another option to improve total device performance is to tune the reflection band not only to the emission wavelength but

Table 3. Calculated external photon efficiency (η_{ext}) for 20 μm cell containing 0.1 wt% K160 in E7 and for the same cell coated with RH- and LH-cholesteric layers centered at 600 nm on both top and bottom as a function of electrical potential applied to the cell and estimated average tilt angle of the dyes, and the calculated relative improvement upon adding the cholesteric reflectors.

Applied potential (V)	0	1	2	3	4	5	6	7	8	9	10
Estimated avg. tilt angle (°)	0	0	25.5	53.6	67.2	73.3	76.6	78.6	79.9	80.8	81.5
ηext - K160 dye alone (%)	2.2	2.2	2.1	1.9	1.8	1.7	1.6	1.6	1.6	1.5	1.5
ηext - with 600 nm cholesteric (%)	2.9	2.9	2.9	2.7	2.6	2.5	2.5	2.4	2.4	2.4	2.4
Increase (%)	33.8	33.2	35.3	43.2	47.7	51.7	53.2	54.2	55.5	56.1	57.1

taking into consideration the path taken by the sun across the sky. Yet another option is to broaden the reflection band of the cholesteric, thereby more effectively covering the complete spectral width of dye emission.[51] Finally, the angular impact of the ChLCs may be reduced by making use of tilt-aligned LCs with anisotropic reflection spectra.[52]

4. Conclusion

PMMA plates coated with static 0.25 wt% coumarin-derivative dye layers and right-handed and left-handed ChLC layers attached directly to the top and bottom surfaces showed edge photon emission increased by up to 30% with ChLC central reflection wavelengths shifted ≈70 nm from the peak emission wavelength of the dye compared to the same sample without the selective reflectors. Adding similar reflectors to switchable LC cells with 0.1 wt% of the same coumarin dye showed increased edge emission an average of ≈35% with a similar red shift in the reflection band with respect to the emission peak wavelength found in the static samples, the fractional increase slightly larger as the tilt angle was increased by applying an electrical potential across the cell.

The use of directly attached ChLC reflectors could significantly improve the viability and cost-effectiveness of LSCs. As research continues into more effective luminophores with enhanced Stokes shifts and quantum yields, the impact of the cholesteric layers can only be enhanced as they effectively restrict surface losses and turn them into meaningful output: current LSCs with efficiencies of 2.22%–6.87% have been produced,[53] and this work suggests this output could be increased to 2.9%–8.9% or more. By improving electrical performance and adding the aesthetic advantages of structural coloration to a wide variety of functional devices, the LSC can be brought closer to effective commercialization. Looking ahead, future research should delve into the further optimization, scalability, and design of these devices to promote their adoption within architectural settings and advance the development of alternative sustainable energy solutions.

Supporting Information

Supporting Information is available from the Wiley Online Library or from the author.

Conflict of Interest

The authors declare no conflict of interest.

Data Availability Statement

The data that support the findings of this study are available from the corresponding author upon reasonable request.

Keywords

chiral nematic (cholesteric) liquid crystals, liquid crystals, luminescent solar concentrators, photonic layers, "smart" window

Received: April 28, 2025
Revised: July 25, 2025
Published online:

[1] A. Anctil, M. N. Beattie, C. Case, A. Chaudhary, B. D. Chrysler, M. G. Debije, S. Essig, D. K. Ferry, V. E. Ferry, M. Freitag, I. Gould, K. Hinzer, H. Hoppe, O. Inganäs, L. Krishnan Jagadamma, M. Hun Jee, R. K. Kostuk, D. Kirk, S. Kube, M. Lim, J. M. Luther, L. Mansfield, M. D. McGehee, D. Nguyen Minh, P. Nain, M. O. Reese, A. Reinders, I. D. W. Samuel, W. van Sark, H. Savin, et al., *J. Photonics Energy* **2023**, *13*, 42301.
[2] P. G. V. Sampaio, M. O. A. González, *Renewable Sustainable Energy Rev.* **2017**, *74*, 590.
[3] M. G. Debije, P. P. C. Verbunt, *Adv. Energy Mater.* **2012**, *2*, 12.
[4] I. Papakonstantinou, M. Portnoi, M. G. Debije, *Adv. Energy Mater.* **2021**, *11*, 2002883.
[5] B. McKenna, R. C. Evans, *Adv. Mater.* **2017**, *29*, 1606491.
[6] C. Stanley, A. Mojiri, G. Rosengarten, *Nanophotonics* **2016**, *5*, 161.
[7] B. S. Richards, I. A. Howard, *Energy Environ. Sci.* **2023**, *16*, 3214.
[8] C. Yang, R. R. Lunt, *Adv. Opt. Mater.* **2017**, *5*, 1600851.
[9] I. Sychugov, *Appl. Opt.* **2020**, *59*, 5715.
[10] M. G. Debije, C. Tzikas, V. A. Rajkumar, M. M. de Jong, *Renew. Energ.* **2017**, *113*, 1288.
[11] W. Eggink, A. Reinders, Design It with LSCs; an Exploration of Applications for Luminescent Solar Concentrator PV Technologies. In 2017 IEEE 44th Photovoltaic Specialist Conference (PVSC) **2017**, pp. 2109–2113. https://doi.org/10.1109/PVSC.2017.8366790.
[12] W. Ma, W. Li, M. Cao, R. Liu, X. Zhao, X. Gong, *Org. Electron.* **2019**, *73*, 226.
[13] A. R. M. Velarde, E. R. Bartlett, N. S. Makarov, C. Castañeda, A. Jackson, K. Ramasamy, M. R. Bergren, H. McDaniel, *ACS Appl. Energy Mater.* **2020**, *3*, 8159.
[14] Y. Zhao, G. A. Meek, B. G. Levine, R. R. Lunt, *Adv. Opt. Mater.* **2014**, *2*, 606.
[15] I. Motta, G. Bottaro, M. Rando, M. Rancan, R. Seraglia, L. Armelao, *J. Mater. Chem. A* **2024**, *12*, 22516.
[16] A. Jaglarz, *Buildings* **2023**, *13*, 2000.
[17] M. N. Gorzaldini, *Mediterr. J. Soc. Sci.* **2016**, *7*, 225.

[18] Z. Qi, J. Li, X. Yang, Z. He, *Comput. Urban Sci.* **2025**, *5*, 7.
[19] L. H. Slooff, E. E. Bende, A. R. Burgers, T. Budel, M. Pravettoni, R. P. Kenny, E. D. Dunlop, A. Büchtemann, *Phys. Status Solidi RRL* **2008**, *2*, 257.
[20] G. Panzeri, E. Tatsi, G. Griffini, L. Magagnin, *ACS Appl. Energy Mater.* **2020**, *3*, 1665.
[21] T. M. Masson, S. D. A. Zondag, K. P. L. Kuijpers, D. Cambié, M. G. Debije, T. Noël, *ChemSusChem* **2021**, *14*, 5417.
[22] M. G. Debije, *Adv. Funct. Mater.* **2010**, *20*, 1498.
[23] C. Han, J. Lee, C. An, S. Oh, *Appl. Mater. Today* **2023**, *35*, 101923.
[24] P. P. C. Verbunt, T. M. de Jong, D. K. G. de Boer, D. J. Broer, M. G. Debije, *Eur. Phys. J. Appl. Phys.* **2014**, *67*, 10201.
[25] M. A. Cardoso, S. F. H. Correia, A. R. Frias, H. M. R. Gonçalves, R. F. P. Pereira, S. C. Nunes, M. Armand, P. S. André, V. de Zea Bermudez, R. A. S. Ferreira, *J. Rare Earths* **2020**, *38*, 531.
[26] M. E. Loik, S. A. Carter, G. Alers, C. E. Wade, D. Shugar, C. Corrado, D. Jokerst, C. Kitayama, *Earth's Future* **2017**, *5*, 1044.
[27] O. Essahili, M. Ouafi, O. Moudam, *Sol. Energy* **2022**, *245*, 58.
[28] C. L. Mulder, P. D. Reusswig, A. M. Velázquez, H. Kim, C. Rotschild, M. A. Baldo, *Opt. Express* **2010**, *18*, A79.
[29] R. W. MacQueen, Y. Y. Cheng, R. G. C. R. Clady, T. W. Schmidt, *Opt. Express* **2010**, *18*, A161.
[30] P. P. C. Verbunt, C. Sánchez-Somolinos, D. J. Broer, M. G. Debije, in *Optics InfoBase Conference Papers*, OSA, Washington, D.C. **2012**, *21*, p. A485.
[31] G. Calzaferri, H. Li, D. Brühwiler, *Chem. – Eur. J.* **2008**, *14*, 7442.
[32] C. L. Mulder, L. Theogarajan, M. Currie, J. K. Mapel, M. A. Baldo, M. Vaughn, P. Willard, B. D. Bruce, M. W. Moss, C. E. McLain, J. P. Morseman, *Adv. Mater.* **2009**, *21*, 3181.
[33] A. M. Kendhale, A. P. H. J. Schenning, M. G. Debije, *J. Mater. Chem. A* **2013**, *1*, 229.
[34] C. Tummeltshammer, A. Taylor, A. J. Kenyon, I. Papakonstantinou, *J. Appl. Phys.* **2014**, *116*, 1.
[35] B. S. Richards, A. Shalav, R. P. Corkish, A Low Escape-Cone-Loss Luminescent Solar Concentrator. In *Proceedings of the 19th European Photovoltaic Solar Energy Conference*; Paris, France **2004**; pp 113–116.
[36] R. Connell, V. E. Ferry, *J. Phys. Chem. C* **2016**, *120*, 20991.
[37] L. Xu, Y. Yao, N. D. Bronstein, L. Li, A. P. Alivisatos, R. G. Nuzzo, *ACS Photonics* **2016**, *3*, 278.
[38] H.-J. Song, B. G. Jeong, J. Lim, D. C. Lee, W. K. Bae, V. I. Klimov, *Nano Lett.* **2018**, *18*, 395.
[39] J. Wang, Y. Yuan, H. Zhu, T. Cai, Y. Fang, O. Chen, *Nano Energy* **2020**, *67*, 104217.
[40] J. C. Goldschmidt, M. Peters, A. Bösch, H. Helmers, F. Dimroth, S. W. Glunz, G. P. Willeke, *Sol. Energy Mater. Sol. Cells* **2009**, *93*, 176.
[41] V. A. Belyakov, E. D. Vladimir, V. P. Orlov, *Sov. Phys. Uspekhi* **1979**, *22*, 64.
[42] M. J. Cook, M. R. Wilson, *J. Chem. Phys.* **2000**, *112*, 1560.
[43] M. G. Debije, M.-P. P. Van, P. P. C. Verbunt, M. J. Kastelijn, R. H. L. Van Der Blom, D. J. Broer, C. W. M. Bastiaansen, *Appl. Opt.* **2010**, *49*, 745.
[44] P. P. C. Verbunt, S. Tsoi, M. G. Debije, D. J. Boer, C. W. M. Bastiaansen, C.-W. Lin, D. K. G. de Boer, *Opt. Express* **2012**, *20*, A655.
[45] G. H. Timmermans, M. van der Heijden, B. M. Oosterlaken, S. C. J. J. Meskers, A. P. H. J. Schenning, M. G. Debije, *ACS Appl. Nano Mater.* **2020**, *3*, 3904.
[46] M. G. Debije, R. C. Evans, G. Griffini, *Energy Environ. Sci.* **2021**, *14*, 293.
[47] C. Yang, H. A. Atwater, M. A. Baldo, D. Baran, C. J. Barile, M. C. Barr, M. Bates, M. G. Bawendi, M. R. Bergren, B. Borhan, C. J. Brabec, S. Brovelli, V. Bulović, P. Ceroni, M. G. Debije, J.-M. Delgado-Sanchez, W.-J. Dong, P. M. Duxbury, R. C. Evans, S. R. Forrest, D. R. Gamelin, N. C. Giebink, X. Gong, G. Griffini, F. Guo, C. K. Herrera, A. W. Y. Ho-Baillie, R. J. Holmes, S.-K. Hong, T. Kirchartz, et al., *Joule* **2022**, *6*, 8.
[48] D. K. G. de Boer, C.-W. Lin, M. P. Giesbers, H. J. Cornelissen, M. G. Debije, P. P. C. Verbunt, D. J. Broer, *Appl. Phys. Lett.* **2011**, *98*, 2.
[49] M. G. Debije, J.-P. Teunissen, M. J. Kastelijn, P. P. C. Verbunt, C. W. M. Bastiaansen, *Sol. Energy Mater. Sol. Cells* **2009**, *93*, 1345.
[50] P. P. C. Verbunt, D. K. G. de Boer, D. J. Broer, M. G. Debije, Special Dispersion Chiral Nematic Reflectors for Luminescent Solar Concentrators. In 2015 IEEE 42nd Photovoltaic Specialist Conference (PVSC); IEEE **2015**; pp. 1–6, https://doi.org/10.1109/PVSC.2015.7355930.
[51] D. J. Broer, J. Lub, G. N. Mol, *Nature* **1995**, *378*, 467.
[52] J. A. H. P. Sol, A. P. H. J. Schenning, M. G. Debije, in *Emerging Liquid Crystal Technologies XVII*, (Eds: I. Muševič, L.-C. Chien, N. V. Tabiryan) SPIE, San Francisco, California, United States **2022**, *12023*, 23, https://doi.org/10.1117/12.2607257.
[53] J. Li, H. Zhao, X. Zhao, X. Gong, *Adv. Funct. Mater.* **2024**, *34*, 2404473.